

Conformational Effects in Photoelectron Spectra of Tetrasilanes

Roman Imhof, Dean Antic, Donald E. David, and Josef Michl*

Department of Chemistry and Biochemistry, University of Colorado, Boulder, Colorado 80309-0215

Received: February 25, 1997; In Final Form: April 11, 1997[⊗]

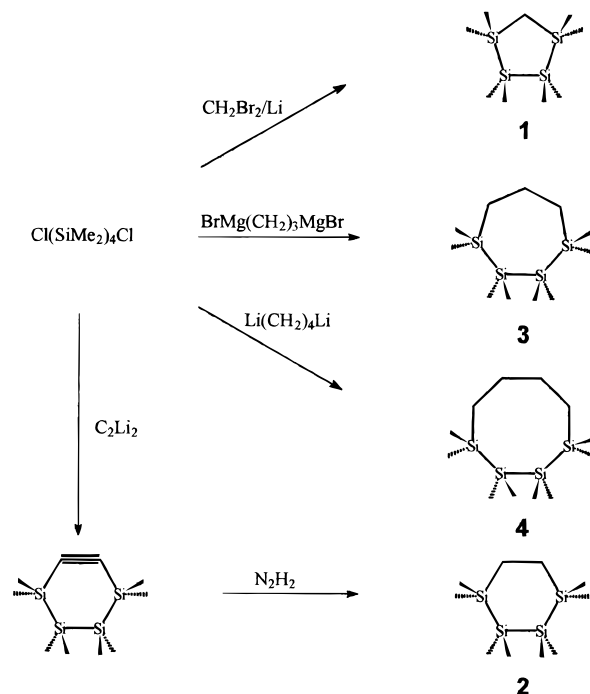
Four cyclic carbosilanes [(SiMe₂)₄(CH₂)_n], *n* = 1–4 (**1–4**), have been synthesized and used as models of conformationally constrained tetrasilane. Results of matrix isolation IR spectroscopy, annealing, and photodestruction, combined with HF/3-21G* calculations on low-energy conformers, suggest that in each compound the SiSiSiSi dihedral angle ω is constrained within relatively narrow limits: **1**, 0°; **2**, 35–55°; **3**, 45–65° (30° for a higher-energy conformer); and **4**, 60–80°. It is argued that other structural differences between **1–4** and the linear chain analogue, decamethyltetrasilane Si₄Me₁₀ (**5**), are of secondary importance, that Koopmans' theorem can be used within a family of closely related structures, and that measurements of photoelectron spectra of **1–5** permit the construction of an experimental counterpart to the orbital energy correlation diagram for the syn–anti conformational transformation in tetrasilane. The trends found for the first three ionization potentials, assigned to electron removal from the three σ_{SiSi} molecular orbitals, are readily understood qualitatively by reference to the ladder C model of saturated chain structure. They show clearly that the even simpler Sandorfy C model is not appropriate for the description of σ conjugation in saturated systems.

Introduction

The unusual properties of saturated polysilane polymers, (SiRR')_x, have attracted considerable attention.^{1–3} In room temperature solution, the polymer chains are coiled and are believed to be segmented into a series of nearly independent oligosilane backbone units communicating enough to permit rapid charge and energy transfer. It is thought that the segmentation is dictated by irregularities in backbone conformation. It has been generally believed that the all-anti conformers have the lowest ionization potentials and excitation energies, and that the local positive charge localization regions (“electrophores”) and chromophores are all-anti chain segments separated by one or more gauche links. In an effort to develop a good understanding of the electronic structure of these polymers we have been examining the shorter chain analogues, the linear oligosilanes Si_nMe_{2n+2}, *n* = 2–16,^{4–8} and found some surprises. Thus, a rough separation of the UV absorption spectra of the individual conformers of two tetrasilanes showed^{7,8} that the first singlet excitation energies of the twisted and the anti conformers do not differ significantly, although the corresponding intensities do, against prior expectations but in agreement with recent calculations.⁶

These results have prompted us to examine the conformational dependence of the electronic structure of tetrasilane more closely. We start by an examination of photoelectron spectra, which provide a relatively simple probe of orbital energies if Koopmans' theorem can be applied, and avoid potential complications due to configuration interaction, expected⁶ to plague interpretations of electronic spectra. In order to minimize ambiguities due to the presence of conformer mixtures in the experimental study, we have chosen the conformationally constrained cyclic tetrasilanes (SiMe₂)₄(CH₂)_n, *n* = 1–4, (**1–4**) in addition to the previously studied⁹ linear chain Si₄Me₁₀ (**5**), whose room-temperature vapor is believed to contain three conformers with very different dihedral angles, ~53°, ~92°, and ~162°.⁷ In each of the cyclic structures, the SiSiSiSi dihedral angle ω can be expected to be constrained to a narrow

SCHEME 1



range of well-defined values smaller than 90° even if several conformers are present. This should offer an opportunity to examine directly the conformational dependence of ionization potentials and compare it with a computed orbital energy diagram in the region $0^\circ < \omega < 180^\circ$. Subsequently, we plan to report a study of excited electronic states.

Results

Syntheses. The four cyclocarbotetrasilanes **1–4** were prepared by condensation of 1,4-dichlorooctamethyltetrasilane (**6**)^{10,11} with the corresponding α,ω -dihaloalkanes metalated with lithium or magnesium (Scheme 1). The preparation of the five-membered ring heterocycle **1** was patterned according to the

[⊗] Abstract published in *Advance ACS Abstracts*, June, 1, 1997.

TABLE 1: Calculated (HF/3-21G*) Energies and Equilibrium Angles

compd	conformer	E_{tot} (au)	E_{rel} (kcal mol ⁻¹)	ω (deg) ^a	δ (deg) ^b
1		-1504.1069	0	0	100
2	a	-1542.9215	0	38	105
	b	-1542.9200	0.9	50	103
3	a	-1581.7378	0	55	107
	b	-1581.7355	1.4	62	107, 111
	c	-1581.7350	1.8	43	110, 112
	d	-1581.7336	2.6	30	112
4	a	-1620.5567	0	65	111, 117
	b	-1620.5563	0.3	63	116
	c	-1620.5556	0.7	70	113
	d	-1620.5539	1.8	80	116
5 ^c	a	-1544.0880	0	164	112
	o	-1544.0869	0.9	92	114
	g	-1544.0872	0.7	54	116

^a SiSiSiSi dihedral angle. ^b SiSiSi valence angle. ^c From ref 7.

literature reaction of CH₂Br₂ with a suspension of Li in tetrahydrofuran (THF), followed by the addition of Me₃SiCl, which forms low yields of (Me₃Si)₂CH₂.¹² The yield of **1** was very poor but provided amounts of pure samples sufficient for spectroscopy.¹³ The six-membered ring **2** was prepared by diimide¹⁴ reduction of the known¹¹ 3,3,4,4,5,5,6,6-octamethyl-3,4,5,6-tetrasilacyclohexyne. The seven-membered heterocycle **3** was synthesized from **6** and the double Grignard compound of 1,3-dibromopropane.¹⁵ A reaction of **6** with Li(CH₂)₄Li¹² was used to produce the eight-membered ring **4**. The heterocycles **1**–**4** are all liquid at room temperature. They are stable under laboratory conditions with the exception of **1**, which is oxidized in air. Subsequent gas chromatography–mass spectrometry (GC-MS) analysis suggests that an oxygen atom is inserted to form an oxatetrasilacyclohexane, but the issue was not pursued further.

With the exception of **1**, the desired product always dominated in the reaction mixtures, but small amounts of structurally related impurities were present and were difficult to separate, leading to poor purified yields for all the compounds. The separation of the products from the reaction mixtures was done by preparative GC.

Molecular Geometries. In order to obtain approximate values of the dihedral angle ω in the heterocycles **1**–**4**, we computed their optimized conformations. The starting geometries were adapted from the known equilibrium geometries of cycloalkanes by placing the four adjacent silicon atoms in all possible distinct locations in the ring. They were subjected to a preliminary MM2^{16,17} force field optimization, followed by an unconstrained HF/3-21G* optimization. Finally, a vibrational frequency analysis was done to verify that the stationary points found were true local energy minima. In spite of this moderately diligent search, it is possible that some low-energy conformers have been overlooked, particularly for the larger two rings. However, we believe that our goal, which was to obtain an approximate range of SiSiSiSi dihedral angles possible for each ring size, has been attained. The results are summarized in Table 1 and the stable conformers that have been found are shown in Figures 1–3, viewed along the Si(2)–Si(3) axis. The ring atoms are colored black. A view of **1** perpendicular to the plane of the silicon atoms is also shown.

As shown in Table 1, only one conformer was found for the five-membered ring **1**, with a dihedral angle ω of 0°. The methylene group is located outside of the plane defined by the four silicon atoms, and this species resembles the envelope form of cyclopentane. The SiSiSi valence angle δ is only 100°, distinctly smaller than the 112° value found⁷ for the open chain

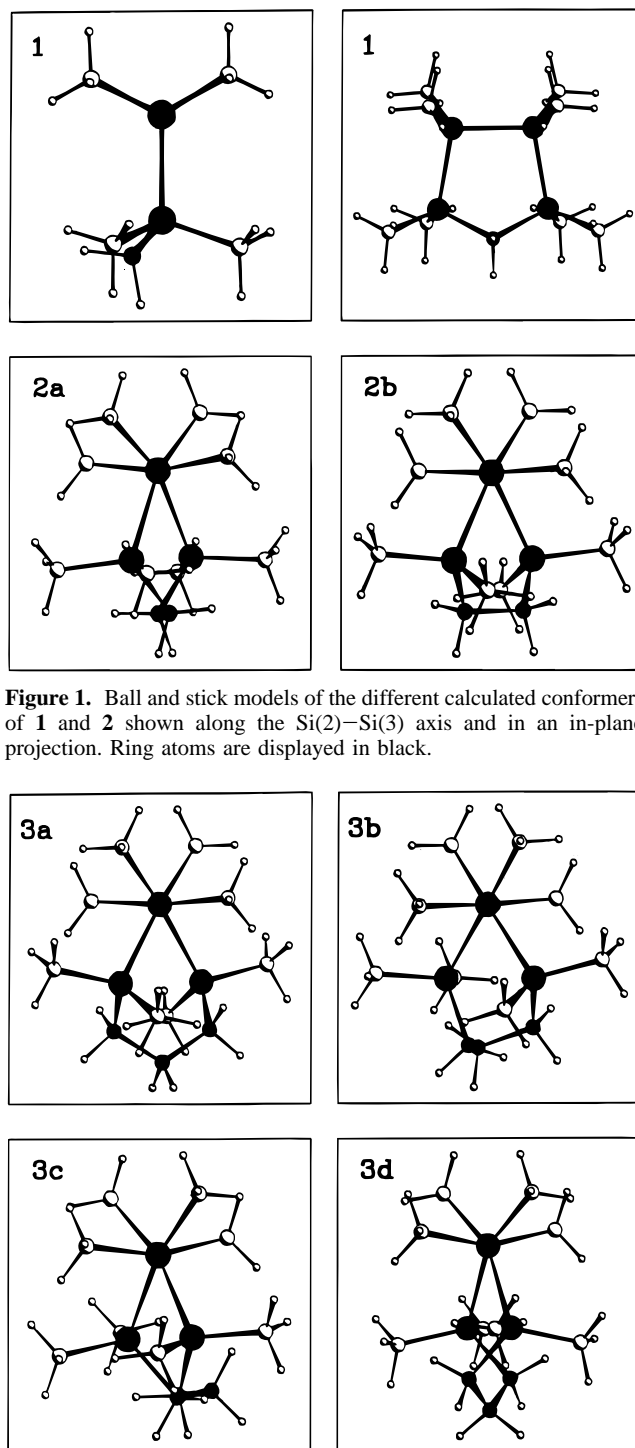


Figure 1. Ball and stick models of the different calculated conformers of **1** and **2** shown along the Si(2)–Si(3) axis and in an in-plane projection. Ring atoms are displayed in black.

Figure 2. Ball and stick models of the different calculated conformers of **3** shown along the Si(2)–Si(3) axis. Ring atoms are displayed in black.

compound **5** at the same level of calculation. For **2**, two stable conformers are predicted. These correspond to the chair and twist-boat conformations in cyclohexane and cyclohexasilane, with the chair slightly more stable. The valence angle δ is still significantly smaller than that in the linear chain **5**. The dihedral angle ω , 38° and 50° in the two conformers, respectively, is smaller than the value calculated for the gauche form of **5**. For each of the larger rings, **3** and **4**, four stable conformers were found, but more could easily be present at room temperature. The valence angles δ and the dihedral angles ω for the most stable conformers are close to the values calculated for the gauche conformer of **5**.⁷

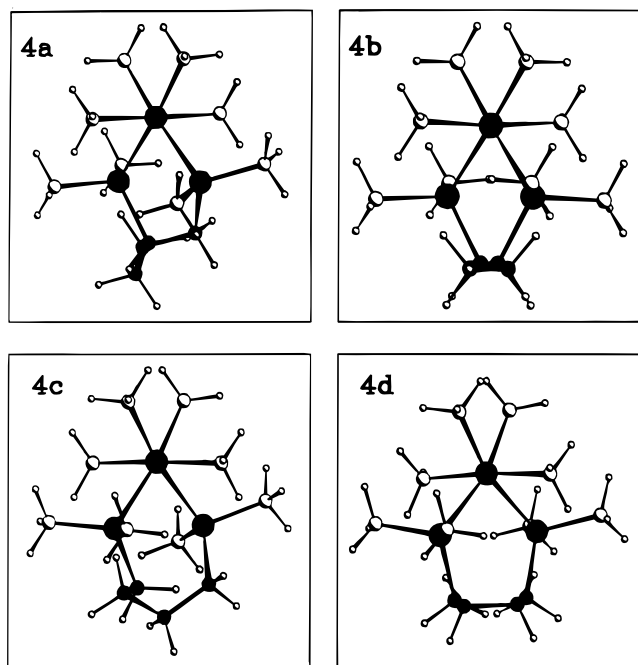


Figure 3. Ball and stick models of the different calculated conformers of **4** shown along the Si(2)–Si(3) axis. Ring atoms are displayed in black.

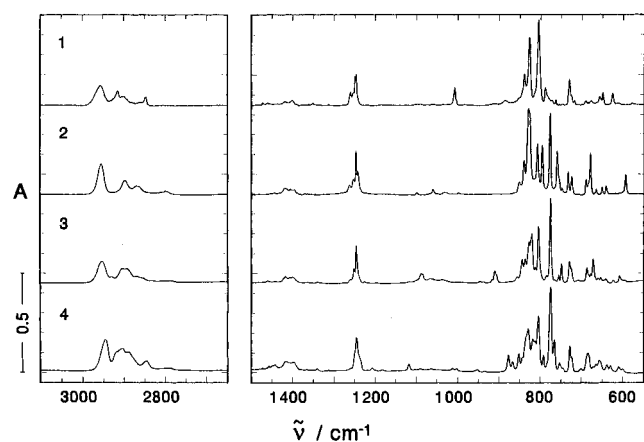


Figure 4. Mid-IR absorption spectra of **1–4**, matrix isolated in Ar at 12 K.

In view of the approximate nature of the computational method and of the possible existence of additional low-energy conformers, possibly differing in the rotation of the methyl substituents only, we believe that these calculations provide only a rough guide to the values of the angles ω and δ in **1–4**. Still, there seems to be little doubt that the species present in a solution or vapor of **1** at room temperature or below have dihedral angles close to 0° and that the corresponding values are $35\text{--}55^\circ$ for **2**, $45\text{--}65^\circ$ for **3** (except for a small amount of **3d**, with $\omega = 30^\circ$), and $60\text{--}80^\circ$ for **4**.

Matrix Isolation IR Spectra. Figure 4 shows the IR spectra of **1–4** in argon matrices. They are very similar to that of **5** and are dominated by absorptions below 1000 cm^{-1} in the region of the SiCH deformation and SiC stretching modes. The numerous CH stretching and CH bending modes in the regions between $2960\text{--}2700$ and $1450\text{--}1200\text{ cm}^{-1}$, respectively, are strongly overlapped.

Encouraged by our previous success in separating the IR spectra of the conformers of Si_4H_{10} ,⁸ and $\text{Si}_4\text{Me}_{10}$,⁷ we attempted a similar analysis for **1–4**. We tried both careful annealing of the matrix and photodecomposition by monochromatic irradiation.

Unlike **5**, the cyclic compounds **1–4** showed at best minor changes in shapes and intensities of their IR bands after careful annealing to 60 K in Xe matrices. The very small variations that were observed were attributed to site rearrangements in the matrix. Deposition of the neat substances allowed annealing up to about 180 K. The molecules are no longer isolated and the absorption bands are broad, but the hope was that this loss of resolution may be outweighed by the larger available temperature range. The spectrum of the five-membered ring compound **1** showed no changes in this experiment, either. This is compatible with the existence of a single conformer. In contrast, the IR spectrum of compound **2** changed substantially and irreversibly, and we conclude that at least two conformers exist. Unfortunately, the pattern of increasing and decreasing IR bands was strongly overlapped, and a reliable separation into the contributions of different conformers was impossible. The spectrum of neat **3** deposited at 12 K had broad peaks and resembled that of the liquid at room temperature. The IR spectrum of **4** changed somewhat upon annealing to 180 K, and the changes were reversible. Thus, the results for **3** and **4** are compatible with the presence of a larger number of conformers of very similar spectral properties.

Our attempts to use monochromatic irradiation at $48\,500\text{ cm}^{-1}$ (iodine lamp), $43\,710\text{ cm}^{-1}$ (Cd lamp), and $39\,420\text{ cm}^{-1}$ (Hg lamp) also failed to help us to separate the spectra of individual conformers. All IR absorption bands of **1–4** decreased in nearly the same ratio in all instances, suggesting that all conformers present have nearly identical absorption and photochemical properties at the three wavelengths used. The nature of the photochemical process is not of particular relevance for the present purposes but seems to be, as anticipated, ring contraction by extrusion of dimethylsilylene. This is suggested by the appearance of a weak IR band at about 1210 cm^{-1} in the initial phases of the irradiation. Upon extended irradiation this band disappears and is replaced with a band at about 2110 cm^{-1} , corresponding to the Si–H stretching mode of 1-methylsilene.¹⁸

In summary, the matrix isolation IR spectral studies support the notion that the rings **1–4** are present either as a single conformer (**1**) or as a mixture of conformers of extremely similar optical and photochemical properties (**2–4**).

Comparison with Calculated IR Spectra. The availability of matrix isolation IR spectra of **1–4** provides an opportunity to check the reliability of the computation of their geometries. Although the self-consistent field (SCF) level of calculation usually reproduces conformational differences quite well¹⁹ and leaves little doubt in the present case, it is reassuring to note that the measured IR spectra agree well with those calculated. The best resolved part of the observed spectra of **1–4** is the region of the SiCH deformation and the SiC stretching modes below 950 cm^{-1} . Figure 5 compares the observed IR spectra of **1–4** in this critical region with the computed IR spectra of all calculated conformers, scaled by a calibration factor of 0.86.

The agreement is best for compound **1**, especially above 750 cm^{-1} . The deviations are larger for the modes that are predominantly of Si–C stretching character. This is in agreement with experience from other systems, including **5**,⁷ where stretching frequencies often require a larger value of the scaling factor than that for deformations in order to agree with the experiment. This suggests that the region between 950 and 750 cm^{-1} is dominated by SiCH deformations and the region below 700 cm^{-1} by SiC stretches. Peaks located between the two regions are assigned mainly to CH_2 deformations. The differences between the frequencies and intensity patterns calculated for the different conformers of each compound are very small, accounting for our failure to separate them spectrally by

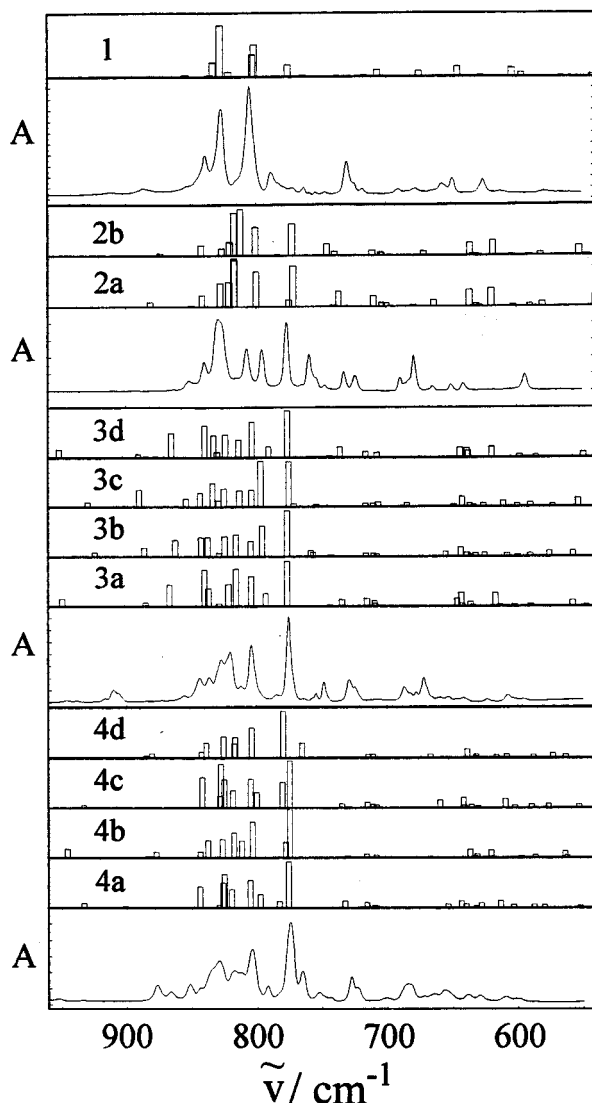


Figure 5. Matrix isolated (Ar, 12 K) and calculated HF/3-21G* IR spectra of the different conformers of 1–4 in the region 950–550 cm^{-1} .

annealing or photodestruction experiments. Once again, we take this to imply a geometrical closeness of the conformers in each case. Thus, we believe that in spite of the degree of conformational flexibility present, the ring compounds 1–4 will be useful for the present purpose as a family of four tetrasilanes with a dihedral angle ω gradually increasing from about 0° to about 80° . We can thus turn to the main subject of this study, an investigation of the effect of this variation in the dihedral angle on the photoelectron spectrum of the tetrasilane moiety.

Photoelectron Spectra. The 7–12 eV region of the He(I) photoelectron spectra of 1–5 is shown in Figure 6 and shows a series of three partially overlapping broad bands, identified by dashed lines (Table 2). Three low-energy bands would be expected, since the molecules contain three easily ionized interacting Si–Si bonds. Above 12 eV, the spectra are featureless and clearly dominated by contributions from the Si–CH₃ groups. The spectrum of 5 agrees with that published earlier.⁹

The bands in the spectra of the cyclic compounds 1–4 are somewhat sharper than those of the linear analogue 5, and it is tempting to assume that the reason for this is that all the conformers of each cyclic compound that are present in significant amounts have similar dihedral angles, while 5 consists of a mixture of three conformers of widely different dihedral angles (at the HF/3-21G* level, the optimized calculated values are 54° for gauche, 92° for ortho, and 164° for anti, and

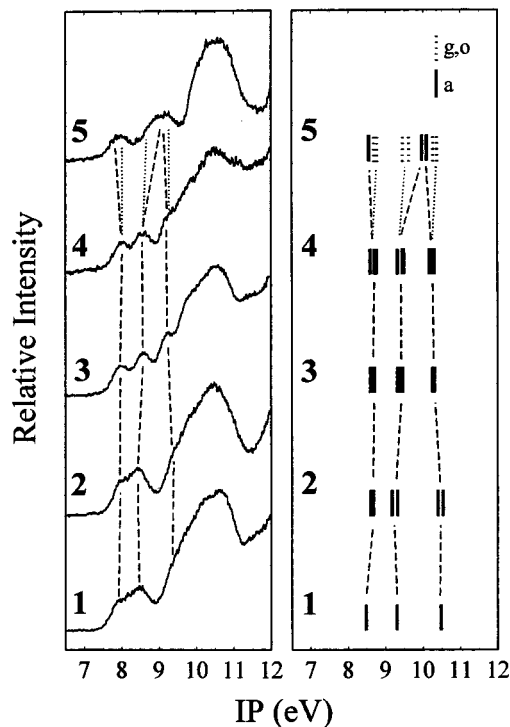


Figure 6. Photoelectron spectra of 1–5: Left, measured; right, calculated for the various conformers (HF/3-21G*, Koopmans' theorem).

TABLE 2: Observed^a and Calculated^b Photoelectron Spectra of 1–5 (eV)

compd	conformer	peak energy ^a or negative orbital energy – 0.95 ^b		
		$1\sigma_{\text{SiSi}}$	$2\sigma_{\text{SiSi}}$	$3\sigma_{\text{SiSi}}$
1		7.9	8.5	~9.3
		7.53	8.35	9.52
2		8.0	8.4	~9.4
	a	<i>7.72</i>	<i>8.21</i>	<i>9.58</i>
3	b	<i>7.64</i>	<i>8.36</i>	<i>9.45</i>
		8.0	8.6	9.2
	a	<i>7.65</i>	<i>8.46</i>	<i>9.30</i>
	b	<i>7.71</i>	<i>8.51</i>	<i>9.30</i>
4	c	<i>7.76</i>	<i>8.43</i>	<i>9.35</i>
	d	<i>7.72</i>	<i>8.37</i>	<i>9.30</i>
		8.0	8.6	9.2
	a	<i>7.64</i>	<i>8.37</i>	<i>9.22</i>
5	b	<i>7.81</i>	<i>8.49</i>	<i>9.35</i>
	c	<i>7.76</i>	<i>8.50</i>	<i>9.31</i>
	d	<i>7.79</i>	<i>8.54</i>	<i>9.35</i>
		~8.0	~9.0	~9.2
	a ^c	<i>7.61</i>	<i>9.03</i>	<i>9.15</i>
	o ^c	<i>7.75</i>	<i>8.68</i>	<i>9.32</i>
	g ^c	<i>7.83</i>	<i>8.51</i>	<i>9.42</i>

^a Boldface. ^b Italic; Koopmans' theorem with additive constant, $-\epsilon(\text{MO}) - 0.95$ eV. ^c Reference 7.

at the MP2/6-31G* level they are 53° , 91° , and 162° , respectively⁷). Also shown in Figure 6 are the ionization potentials expected from HF/3-21G* orbital energies using Koopmans' theorem, calculated at the optimized geometries of all the conformers found for the five compounds (Table 2). They confirm the intuitively expected result in that the ionization potentials of all the conformers of any one of the cyclic compounds are nearly identical, while for 5 the differences are much larger. The molecules are too big for a calculation of ionization energies at a level that goes beyond Koopmans' theorem. In view of their great similarity, this is not likely to hurt a discussion of trends, particularly given the previously

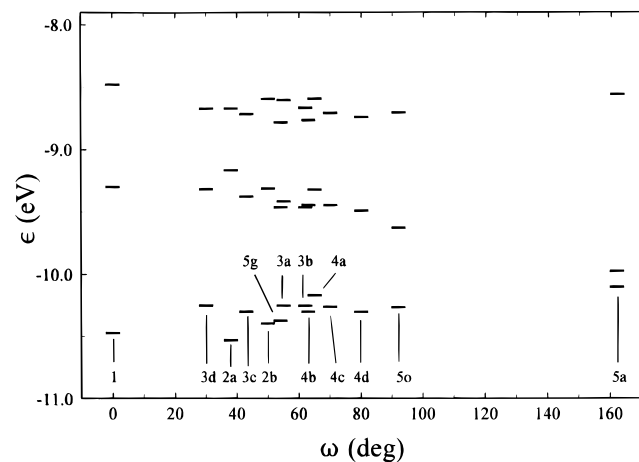


Figure 7. Computed HF/3-21G* molecular orbital energies for the conformers of **1–5**.

found²⁰ resemblance between Koopmans' theorem results and results of correlated calculations for Si₄H₁₀.

Discussion

We believe that the cyclic tetrasilanes **1–4** represent good models for conformationally constrained permethylated tetrasilane **5**. Although more than one conformer of each is surely present in our samples, with the likely exception of **1**, the electronic structure properties of each member of a conformer family are very similar. This follows from the extreme similarity of their matrix isolation IR spectra, the matrix annealing and photodestruction experiments, and agrees with the narrower width of bands in the photoelectron spectra of **1–4** compared with those of **5**, which undoubtedly is a mixture of conformers that differ considerably in their dihedral angles. As argued in the Results section, the *ab initio* calculations leave little doubt that **1** is representative of a peralkylated tetrasilane with a dihedral angle ω near 0°, **2** of one with ω equal to $45 \pm 10^\circ$, **3** of one with ω equal to $55 \pm 10^\circ$ (except for the presumably minor amount of a conformer with $\omega = 30^\circ$), and **4** of one with ω equal to $70 \pm 10^\circ$.

Unfortunately, the valence angles δ certainly also vary throughout the series. Prior computational work²¹ on Si₃H₈ makes it likely that this variation will affect the ionization potentials by up to 0.1 eV. The value of δ is computed to increase from 100 to 117° upon going from **1** to **4** (Table 1) and can be compared with the value of 112° calculated for the open-chain compound **5**. Fortunately for our purposes, Figure 7 shows that the variability of δ and other secondary structural parameters throughout the series **1–5** is indeed calculated to have an effect no larger than about 0.1 V and to have little importance for the general trend computed for molecular orbital energies as a function of ω . The only likely exception is **1**, where a particularly small value of δ is combined with the opportunity for hyperconjugative interaction between the tetrasilane chain ends through a single methylene group. The highest occupied molecular orbital (HOMO) of the σ_{SiSi} type is expected to be symmetric relative to the plane that passes through the three atoms of the CH₂ group, suggesting that interaction with the occupied CH bond orbital of this group will push the HOMO to higher energy and reduce the first ionization potential somewhat.

The availability of observations for **1–4** permits us to produce an experimental counterpart to nearly one half of the total correlation diagram between the syn and anti limits of tetrasilane conformation. It would be ideal to obtain similar access to the

second half as well, but the design and synthesis of tetrasilane conformers constrained to angles ω between 90 and 180° are more difficult. Unlike the UV absorption spectrum of the pure anti conformer of **5**, which was derived from the prior matrix isolation work fairly reliably,⁷ the photoelectron spectrum in Figure 6 is only available as a superposition of contributions from all three conformers. If we make the reasonable assumption that the gauche and ortho contributions to the superposition can be approximated by the spectra of **3** and **4**, we can estimate what the photoelectron spectrum of the pure anti form would have to look like in order to produce the superposition spectrum observed for **5**. It seems that the first ionization peak of pure anti **5** has to occur about 0.1–0.2 eV lower than that of **4** and that its second and third ionization potentials must be very close and have to lie about 0.1–0.2 eV below the third ionization potential of **4**, and this is indicated by the dashed lines in Figure 6.

In spite of the moderate reservations expressed above, it appears reasonable to propose that as ω grows from 0 to 180°, the observed first and third ionization potentials drop very slightly, by 0.1 or 0.2 eV, and the second ionization potential increases more substantially, by perhaps 0.5–0.7 eV. Certainly, the increase in the separation of the first and second peaks in the spectrum is unmistakable. Most of the change seems to occur upon going from **4** to **5**, i.e., for $\omega > 70^\circ$, and this emphasizes anew the need for a future synthesis of tetrasilanes constrained to these large dihedral angles.

Regardless of the well-recognized inadequacies of Koopmans' theorem, the agreement with the trends computed for orbital energies, also shown in Figure 6, is excellent, even though all calculated absolute magnitudes would have to be shifted by about 0.95 eV to lower energies to get numerical agreement. This does not come as a surprise since similar agreement in trends was reported earlier²⁰ between Koopmans' theorem results and electron propagator results on a related molecule, Si₄H₁₀. The present calculations confirm the suspected assignment of the three low-energy peaks to the three σ_{SiSi} molecular orbitals. In **1–4**, their energy order is computed to be a, b, a, using labels appropriate for C₂ symmetry.

This is the order that would be expected from the Sandorfy C model,²² in which tetrasilane is isoelectronic with 1,3,5-hexatriene, the lowest energy σ_{SiSi} molecular orbital is an in-phase combination of the three σ bond orbitals and has no nodes through Si atoms, the next one is the antisymmetric combination of the terminal σ bond orbitals, and the highest energy orbital is a combination of the three σ bond orbitals that has a node through each of the internal Si atoms. In this model, the splitting of the orbital energies as the σ bond orbitals combine into σ_{SiSi} molecular orbitals is due to the geminal resonance integral between two backbone sp³ hybrids on the same Si atom. Since neither this integral nor the vicinal resonance integral that causes the splitting of σ bond and σ^* antibond orbitals are a function of ω , no conformational dependence of the photoelectron spectrum whatever is predicted. This is clearly wrong. A remedy was sought in the recognition of the existence of "perivalent" resonance integrals between sp³ hybrids located on adjacent Si atoms and pointed at an angle away from each other.⁵ The introduction of these additional interactions converts the topology of the sp³ hybrid orbital system from linearly conjugated to ladder conjugated, and this improvement of the Sandorfy model was therefore dubbed "ladder C" model. Since the perivalent interactions depend on an overlap that is largely of π type, they vary considerably as a function of ω and the resonance integral even changes sign from negative at the syn conformation to positive at the anti conformation.

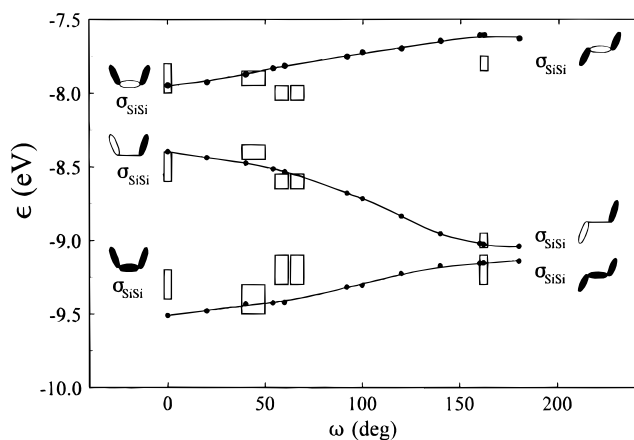


Figure 8. Computed (HF/3-21G*) molecular orbital energies of **5**, shifted to less negative values by 0.95 eV, as a function of dihedral angle ω (all other geometrical variables have been optimized). The rectangles show the orbital energies estimated from photoelectron spectra observed for **1–5**, using Koopmans' theorem, plotted against the most likely dihedral angles.

As shown in the computed (HF/3-21G*) orbital energy diagram in Figure 8, the observed qualitative trends are accounted for perfectly by the ladder C description when the perivalent interaction is thought of as a perturbation. The coefficients on the two sp^3 hybrids in question are of the opposite signs in the second molecular orbital and of equal signs in the first and the third. Thus, at the syn geometry, the introduction of the negative perivalent resonance integral is stabilizing in the first and third orbital and destabilizing in the second orbital, and the opposite is true at the anti geometry where the resonance integral is positive. The effects are larger for the second orbital, since it has the largest coefficients on the sp^3 hybrids involved (because of its symmetry, this molecular orbital does not contain any contribution from the central σ_{SiSi} bond orbital). These qualitative considerations have already appeared in literature in more detail.²⁰

We conclude first that the observed trends make intuitive sense and second that the energy effects of the perivalent type of interaction actually are comparable with those of the geminal type. As a result, attempts to understand σ conjugation in terms of the latter alone, intrinsic to the popular Sandorfy C model, are of questionable value.

Conclusion

The synthesis of the cyclic carbosilanes **1–4** and the investigation of their vibrational spectra under conditions of matrix isolation, annealing, and photodestruction, combined with ab initio optimization of their geometries, provided a basis for constructing an experimental counterpart to about half of the orbital energy correlation diagram for the conformational syn–anti transformation in tetrasilane. It demonstrated that the ionization potential of the syn form is only about 0.1–0.2 eV higher than that of the anti form, while the variation is much larger for the second highest molecular orbital. The observed trends are in excellent agreement with HF/3-21G* calculations employing Koopmans' theorem, but also with the simple ladder C model, and permit the conclusion that perivalent and geminal interactions are of comparable importance. This invalidates the use of the even simpler Sandorfy C model for the description of σ conjugation in saturated silicon chains.

It is now known^{6–8} that even the ladder C model is inadequate for the interpretation of the properties of electronically excited states because it ignores interactions with the lateral bonds on the Si atoms, but at least for tetrasilane, this model works fine

when ionization energies alone are considered. It is possible that it will prove useful for modeling hole conduction through variously coiled polysilane chains.

Experimental Section

Materials and Methods. Commercial solvents were dried before use. Decamethyltetrasilane **5** was prepared according to a literature procedure.²³ All samples were purified by preparative gas chromatography, performed with a Varian 3400 Gas Chromatograph on a 6 ft \times 1/4 in. SE-52 CW-HP 80/100 standard packed column from Baxter using a temperature ramp from 80 to 250 °C. Proton and carbon magnetic resonance spectra were taken on a Varian VXR 300 S spectrometer. UV spectra were measured with a Cary 17 spectrophotometer modified by Olis, Inc. Mid-IR spectra were measured at 1 cm^{-1} resolution on a Nicolet 800 FTIR spectrometer equipped with a wide-range nitrogen-cooled mercury cadmium telluride detector. Mass spectra were measured with a VG 7070EQ-HF (VG Instruments, Manchester) double focusing mass spectrometer at an ionizing voltage of 70 eV and a HP5988A (Hewlett Packard) GC-MS. Elemental analyses were performed by Desert Analytics, Tucson, AZ. Photoelectron spectra were measured on a home-built instrument similar to a Perkin-Elmer model PS-18. Resolution was about 30 meV, and the reported peak positions are thought to be accurate to within 20 meV. MM2 force field calculations were done with the programs SPARTAN¹⁶ and MOLGEN.¹⁷ Quantum mechanical calculations were done at the Hartree-Fock level using a 3-21 G* basis set with an IBM RS6000-550 workstation with Gaussian92.²⁴

Matrix Isolation. Argon, nitrogen (US Welding, 99.999% purity), or xenon (Spectra Gases Inc., 99.99% purity) was deposited on a CsI window mounted on the second stage of a closed-cycle helium refrigerator (Air Products Displex 202) in an oxygen-free copper sample holder, which was maintained at 12 K during the deposition. Samples were evaporated from a reservoir held at -20 – -40 °C into the stream of inert gas at a flow rate of about 2 mmol/h, producing matrices with matrix ratios estimated to be about 1:1000. The matrix was irradiated at 12 K either with a low-pressure cadmium spectral lamp (Philips 93107E; 43 710 cm^{-1}) or with a home-built microwave-powered low-pressure iodine lamp (48 500 cm^{-1}) with a Suprasil quartz window. For some experiments with compound **1**, a low-pressure mercury lamp (Philips 93109E, 39 420 cm^{-1}) was used. A 1 in. air-saturated water filter was used with all three lamps to reduce the heat load on the sample and to block unwanted 56 090 cm^{-1} radiation from the iodine lamp.

Synthesis. 1,4-Dihydrooctamethyltetrasilane, H(SiMe₂)₄H. This compound was prepared according to a description provided by Barton et al.¹¹ Typically, to a 250 mL three-necked argon-flushed round bottomed flask, which was equipped with a magnetic stirrer and a dropping funnel, was added freshly distilled THF (120 mL) and lithium wire (4.5 g, 0.64 mol, 3.2 mm, Aldrich). A mixture of dimethyldichlorosilane (20 mL, 0.16 mol) and dimethylchlorosilane (40 mL, 0.36 mol) was slowly added dropwise into the lithium suspension while the flask was cooled by an ice-water bath, and the lithium suspension was vigorously stirred. After complete addition the reaction mixture was allowed to warm up to room temperature and was stirred overnight. Pentane (50 mL) was added and the salt removed by filtration under inert atmosphere. After the solvent was evaporated, a clear yellow liquid remained from which H(SiMe₂)₄H (1 g, 4.2 mmol) was separated by fractional distillation (1.5 Torr/55 °C). ¹H NMR (CDCl₃, 300 MHz): δ 3.729 (sept, 2 H), 0.137 (d, 12 H), 0.136 (s, 12 H).

1,4-Dichlorooctamethyltetrasilane, Cl(SiMe₂)₄Cl (6**).**¹⁰ This compound was prepared according to a description provided

by Barton et al.¹¹ To an oven-dried, argon-flushed 50 mL flask, equipped with a magnetic stirrer and a condenser, were added H(SiMe₂)₄H (1 g, 4.2 mmol), CCl₄ (20 mL), and benzoyl peroxide (5 mg, 0.03 mmol). The mixture was refluxed overnight under argon atmosphere to give **6** in quantitative yield. The solvent was removed in a rotary evaporator. ¹H NMR (CDCl₃, 300 MHz): δ 0.51 (s, 12 H), 0.25 (s, 12 H).

1,1,2,2,3,3,4,4-Octamethyltetrasilacyclopentane (1). Freshly distilled THF (10 mL) and Li wire (50 mg, 7.1 mmol, 3.2 mm, Aldrich) were placed into a 25 mL flask held under a positive pressure of Ar. The mixture was cooled down to 0 °C, and 3 mL of a solution of CH₂Br₂ (0.2 mL, 1.8 mmol) and **6** (0.5 g, 1.7 mmol) in THF (5 mL) was added quickly. The rest of this solution was added slowly over 10 min. The reaction mixture turned pale yellow, and the Li wire was completely consumed. The mixture was allowed to warm up overnight, the solvent evaporated, and the residue dissolved in pentane. The solution was then poured on ice and washed with ice-cold water (3 × 10 mL). The organic layer was separated and dried over CaCl₂. After filtration and evaporation of the solvent, there remained a yellow brown oil from which **1** was separated by preparative GC to give 1 mg (4 μmol, 0.2%) of a pure liquid. UV (hexane): 38 700 (sh, 300), 42 500 (3700), 47 500 (sh, 8500) cm⁻¹. IR (neat): 2953 (s), 2912 (m), 2895 (w), 1401 (w), 1255 (sh), 1249 (s), 1037 (s), 907 (w), 881 (w), 827 (s), 801 (vs), 770 (s), 730 (w), 684 (w), 663 (w) cm⁻¹. ¹H NMR (CDCl₃, 300 MHz): δ 0.117 (s, 12 H), 0.074 (s, 12 H), -0.218 (s, 2 H). ¹³C NMR (75 MHz, CDCl₃): δ 3.461, -0.844, -7.056. MS: *m/z* 246 (M⁺, 32), 73 (SiMe₃⁺, 100). HRMS calcd 246.1112, obsd 246.1123.

1,1,2,2,3,3,4,4-Octamethyl-1,2,3,4-tetrasilacyclohexane (2). Crude 3,3,4,4,5,5,6,6-octamethyltetrasilacyclohexyne¹¹ (1 g) was dissolved in hexane, (15 mL) and potassium azodicarboxylate¹⁴ (1.55 g, 8 mmol) was added. A solution of acetic acid (0.48 g, 8 mmol) in 1,4-dioxane (15 mL) was added slowly, and the reaction mixture was stirred for 2 h at room temperature. The solution was poured into an ice water/hexane mixture (1:1) and washed with ice-cold water (3 × 10 mL). The organic layer was separated and dried over CaCl₂. After filtration and evaporation of the solvent, a yellowish brown oil remained. The product **2** was isolated from this mixture by preparative GC to give 170 mg (20%) of a pure liquid. UV (hexane): 43 000 (sh, 4500), 46 300 (8500) cm⁻¹; IR (neat): 2950 (m), 2891 (m), 2865 (sh), 2795 (w), 1414 (w), 1404 (w), 1258 (sh), 1245 (s), 1096 (vw), 1061 (vw), 1026 (vw), 999 (vw), 825 (vs), 804 (w), 794 (w), 776 (s), 758 (m), 732 (m), 687 (w), 677 (m), 664 (vw), 648 (vw), 638 (vw), 593 (w). ¹H NMR (CDCl₃, 300 MHz): δ 0.755 (m, 4 H), 0.107 (s, 12 H), 0.015 (s, 12 H) cm⁻¹. ¹³C NMR (75 MHz, CDCl₃): δ 10.187, -3.687, -6.869. MS: *m/z* 260 (M⁺, 51), 232 (M⁺ - C₂H₄, 16), 116 ((Me₂Si)₂⁺, 27), 73 (SiMe₃⁺, 100). HRMS calcd 260.1268, obsd 260.1260. Anal. Calcd for C₁₀H₂₈Si₄: C, 46.15; H, 10.77. Found: C, 45.72; H, 10.61.

1,1,2,2,3,3,4,4-Octamethyl-1,2,3,4-tetrasilacycloheptane (3). Mg (600 mg, 24.9 mmol) was placed into a 25 mL flask and heated for 4 h to 150 °C under Ar. The Ar inlet was replaced by a septum, and the flask was cooled down to room temperature. Et₂O (5 mL) was added, and a solution of Br(CH₂)₃Br (0.63 mL, 6.4 mmol) in Et₂O (7 mL) was added dropwise. To this mixture a solution of **6** (1 g, 3.3 mmol) in Et₂O (5 mL) was added immediately. The reaction mixture was stirred overnight under Ar, poured on ice, and washed with ice-cold water (3 × 10 mL). The organic layer was separated and dried over CaCl₂. After filtration and evaporation of the solvent, a yellow brown oil remained, and **3** was isolated by preparative

GC to give 150 mg (0.54 mmol, 16%) of a pure liquid. UV (hexane): 42 800 (3200), 48 000 (sh, 11 000) cm⁻¹. FTIR (neat): 2947 (s), 2928 (sh), 2899 (s), 2889 (s), 2867 (m), 2852 (m), 2790 (w), 1458 (w), 1412 (m), 1405 (m), 1339 (w), 1245 (s), 1226 (sh), 1091 (m), 1085 (w), 1037 (vw), 944 (vw), 937 (vw), 910 (m), 820 (vs), 803 (s), 776 (vs), 748 (m), 729 (s), 687 (m), 670 (s), 653 (w), 638 (w), 619 (vw), 604 (m), 594 (sh) cm⁻¹. ¹H NMR (CDCl₃, 300 MHz): δ 1.659 (m, 4 H), 0.721 (m, 2 H), 0.104 (s, 12 H), 0.024 (s, 12 H). ¹³C NMR (75 MHz, CDCl₃): δ 19.320, 18.096, -3.272, -6.585. MS: *m/z* 274 (M⁺, 37), 174 ((Me₂Si)₃⁺, 23), 116 ((Me₂Si)₂⁺, 100), 73 (SiMe₃⁺, 80). HRMS calcd 274.1425, obsd 274.1421. Anal. Calcd for C₁₁H₃₀Si₄: C, 48.17; H, 10.95. Found: C, 48.17; H, 11.23.

1,1,2,2,3,3,4,4-Octamethyl-1,2,3,4-tetrasilacyclooctane (4). Freshly distilled Et₂O (20 mL) and Li wire (225 mg, 32 mmol, 3.2 mm, Aldrich) were placed into a 100 mL three-neck flask equipped with a reflux condenser and a dropping funnel and held under a positive pressure of Ar. The mixture was cooled to 0 °C, and 3 mL of a solution of Br(CH₂)₄Br (0.95 mL, 8 mmol) in Et₂O (5 mL) was added quickly. The remainder of this solution was added dropwise over 10 min. Then a solution of **6** (1.5 g, 5 mmol) in Et₂O (40 mL) was added slowly. The reaction mixture was allowed to warm up overnight, poured on ice, and washed with ice-cold water (3 × 10 mL). The organic layer was separated and dried over CaCl₂. After filtration and evaporation of the solvent, a yellow brown oil remained. Pure liquid **4** was isolated by preparative GC (220 mg, 0.76 mmol, 15%). UV (hexane): 43 300 (5100), 49 000 (sh, 15 000) cm⁻¹; FTIR (neat): 2947 (s), 2919 (sh), 2904 (s), 2892 (m), 2849 (m), 2874 (w), 1458 (vw), 1449 (vw), 1444 (vw), 1415 (w), 1405 (w), 1340 (vw), 1246 (s), 1205 (vw), 1119 (vw), 1011 (vw), 1003 (vw), 954 (vw), 876 (w), 865 (w), 846 (sh), 827 (s), 815 (sh), 805 (s), 792 (w), 776 (vs), 754 (sh), 729 (m), 699 (vw), 685 (m), 662 (vw), 655 (w), 637 (vw), 628 (vw), 609 (vw), 597 (vw) cm⁻¹. ¹H NMR (CDCl₃, 300 MHz): δ 1.470 (m, 4H), 0.673 (m, 4H), 0.091 (s, 12H), 0.034 (s, 12H). ¹³C NMR (75 MHz, CDCl₃): δ 26.144, 13.180, -3.133, -6.352. MS: *m/z* 288 (M⁺, 38), 174 ((Me₂Si)₃⁺, 100), 116 ((Me₂Si)₂⁺, 64), 73 (SiMe₃⁺, 65). HRMS calcd 288.1581, obsd 288.1592. Anal. Calcd for C₁₂H₃₂Si₄: C, 50.00; H, 11.11. Found: C, 49.58; H, 11.23.

Acknowledgment. The authors are grateful to the Japan High Polymer Center for support within the framework of the Industrial Science and Technology Frontier Program funded by the New Energy and Industrial Technology Development Organization. R.I. is grateful to the Schweizerischer Nationalfonds zur Förderung der wissenschaftlichen Forschung for a fellowship. We are indebted to Prof. Tom Barton for kindly supplying a detailed description of the synthesis of 3,3,4,4,5,5,6,6-octamethyl-3,4,5,6-tetrasilacyclohexyne.

References and Notes

- (1) Miller, R. D.; Michl, J. *Chem. Rev.* **1989**, *89*, 1359.
- (2) For examples of recent experimental studies, see: Itoh, T.; Mita, I. *Macromolecules* **1992**, *25*, 479. Karikari, E. K.; Greso, A. J.; Farmer, B. L.; Miller, R. D.; Rabolt, J. F. *Macromolecules* **1993**, *26*, 3937. Yuan, C. H.; West, R. *Macromolecules* **1994**, *27*, 629. Sakamoto, K.; Yoshida, M.; Sakurai, H. *Macromolecules* **1994**, *27*, 881.
- (3) For examples of computational studies, see: Cui, C. X.; Karpfen, A.; Kertesz, M. *Macromolecules* **1990**, *23*, 3302. Jalali-Heravi, M.; McManus, S. P.; Zutauf, S. E.; McDonald, J. K. *Chem. Mater.* **1991**, *3*, 1024. Welsh, W. J. *Adv. Polym. Technol.* **1993**, *12*, 379.
- (4) Sun, Y.-P.; Michl, J. *J. Am. Chem. Soc.* **1992**, *114*, 8186. Sun, Y.-P.; Wallraff, G. M.; Miller, R. D.; Michl, J. *J. Photochem. Photobiol.* **1992**, *62*, 333.

- (5) Plitt, H. S.; Downing, J. W.; Raymond, M. K.; Balaji, V.; Michl, J. *J. Chem. Soc., Faraday Trans.* **1994**, *90*, 1653. Plitt, H. S.; Balaji, V.; Michl, J. *Chem. Phys. Lett.* **1993**, *213*, 158. Plitt, H. S.; Michl, J. *Chem. Phys. Lett.* **1992**, *198*, 400.
- (6) Teramae, H.; Michl, J. *Mol. Cryst. Liq. Cryst.* **1994**, *256*, 149.
- (7) Albinsson, B.; Teramae, H.; Downing, J. W.; Michl, J. *Chem. Eur. J.* **1996**, *2*, 529.
- (8) Albinsson, B.; Teramae, H.; Plitt, H. S.; Goss, L. M.; Schmidbaur, H.; Michl, J. *J. Phys. Chem.* **1996**, *100*, 8681.
- (9) Bock, H.; Ensslin, W. *Angew. Chem., Int. Ed. Engl.* **1971**, *10*, 404.
- (10) Sen, P. K.; Ballard, D.; Gilman, H. *J. Organomet. Chem.* **1968**, *15*, 237.
- (11) Barton, T. J. Private communication. Pang, Y.; Schneider, A.; Barton, T. J.; Gordon, M. S.; Carroll, M. T. *J. Am. Chem. Soc.* **1992**, *114*, 4920. Ijadi-Maghsoodi, S.; Pang, Y.; Barton, T. J. *J. Polym. Sci., Part A: Polym. Chem.* **1990**, *28*, 955.
- (12) West, R.; Rochow, E. G. *J. Org. Chem.* **1953**, *18*, 1739.
- (13) During the preparation of this manuscript we learned that Prof. Sakurai and his collaborators have synthesized **1** in larger quantities.
- (14) Hamersma, J. W.; Snyder, E. I. *J. Org. Chem.* **1965**, *30*, 3985.
- (15) Seetz, J. W. F. L.; Hartog, F. A.; Böhm, H. P.; Blomberg, C.; Akkerman, O. S.; Bickelhaupt, F. *Tetrahedron Lett.* **1982**, *23*, 1497.
- (16) *Spartan Version 4.0*; Wavefunction, Inc.: Irvine, CA, 1995.
- (17) Baričič, P.; Mackov, M.; Slone, J. E.; *MOLGEN Version 3.0*; Scientific Consulting Services: Alexandria, VA, 1994.
- (18) Raabe, G.; Vancik, H.; West, R.; Michl, J. *J. Am. Chem. Soc.* **1986**, *108*, 671.
- (19) Clementi, E.; Kistenmacher, H.; Popkie, H. *J. Chem. Phys.* **1973**, *58*, 4699. Hehre, W. J.; Radom, L.; Schleyer, P. v. R.; Pople, J. A. *Ab Initio Molecular Orbital Theory*; Wiley: New York, 1985; p 80.
- (20) Ortiz, J. V.; Mintmire, J. W. *J. Am. Chem. Soc.* **1988**, *110*, 4522. Ortiz, J. V. *J. Chem. Phys.* **1991**, *94*, 6064.
- (21) Ortiz, J. V.; Mintmire, J. W. *J. Phys. Chem.* **1991**, *95*, 8609.
- (22) Sandorfy, C. *Can. J. Chem.* **1955**, *33*, 1337.
- (23) Sakurai, H.; Yamamori, M.; Yamagata, M.; Kumada, M. *Bull. Chem. Soc. Jpn.* **1968**, *41*, 1474.
- (24) Frisch, M. J.; Trucks, G. W.; Head-Gordon, M.; Gill, P. M. W.; Wong, M. W.; Foresman, J. B.; Johnson, B. G.; Schlegel, H. B.; Robb, M. A.; Replogle, E. S.; Gomperts, R.; Andres, J. L.; Raghavachari, K.; Binkley, J. S.; Gonzales, C.; Martin, R. L.; Fox, D. J.; Defrees, D. J.; Baker, J.; Stewart, J. J. P.; Pople, J. A. *Gaussian 92, Revision C*; Gaussian, Inc.: Pittsburgh, PA, 1992.